Two distalization methods compared in a novel patient-specific finite element analysis

Makram J. Ammoury,[a] Samir Mustapha,[b] Paul C. Dechow,[c] and Joseph G. Ghafari[a,d]
Beirut, Lebanon, Dallas, Tex, and Philadelphia, Pa

Introduction: Orthodontic mini-implants aid in the correction of distocclusions via direct anchorage (pull from mini-implant to teeth) and indirect anchorage (teeth pulled against other teeth anchored by the mini-implant). The aim of this study was to compare stress levels on the periodontal ligament (PDL) of maxillary buccal teeth in direct and indirect distalization against orthodontic mini-implants and accounting for individual variation in maxillary anatomy and biomechanical characteristics of the compact bone. **Methods:** A 3D model of the maxilla containing the different components (teeth, PDL, trabecular and cortical bones) was generated from a computed tomographic scan. Cortical bone was divided into several areas according to previously defined zones. Bone stiffness and thickness data, obtained from 11 and 12 cadavers, respectively, were incorporated into the initial model to simulate the individual cortical bone variation at the different locations. Subsequently, a finite element analysis was used to simulate the distalization modalities. **Results:** Stresses at the buccal, palatal, mesial, and distal surfaces were significantly different between adjacent teeth under stiffness but not thickness variation. In both distalization modalities, low or no significant correlations were found between stress values and corresponding cortical bone thicknesses. High significant and inverted correlations were observed at the first molar between stress amounts and cortical bone stiffness (direct modality: $-0.68 < r < -0.72$; indirect modality: $-0.80 < r < -0.82$; $P < 0.05$). **Conclusions:** With the use of a novel finite element approach that integrated human data on variations in bone properties, findings suggested that cortical bone stiffness may influence tooth movement more than bone thickness. Significant clinical implications could be related to these findings. (Am J Orthod Dentofacial Orthop 2019;156:326-36)

Temporary anchorage devices (TADs) significantly facilitate the distal movement of the maxillary buccal teeth, particularly in noncompliant patients who would not properly wear adjunct appliances (eg, headgear), and contribute to the success of nonextraction treatments[1] without anchorage loss.[2] Interradicular buccal TADs are most frequently used because they are easier to anchor and retrieve, and they cause fewer irritations to soft tissues when inserted within the zone of attached gingiva as recommended.[3]

Much knowledge and corresponding clinical applications have emerged from research on implant types, failures, optimal levels of placement, and optimal forces used for tooth movement.[4,5] However, information needed to improve treatment planning is difficult to obtain in human investigation in the oral cavity, namely, the noninvasive quantification of stresses generated in tissues adjacent to the teeth under different anatomic conditions and in response to various biomechanical set-ups. For such computations, the oral environment must be replicated as close as possible to real anatomy and subjected to virtual testing. A primary approach used for such research is finite element analysis (FEA).

FEA is an engineering technique that allows inferences about stress and strain distributions to be made from a mathematical model corresponding to a predetermined set-up or scenario.[6] The method may provide

[a]Division of Orthodontics and Dentofacial Orthopedics, American University of Beirut Medical Center, Beirut, Lebanon.
[b]Department of Mechanical Engineering, Maroun Semaan Faculty of Engineering and Architecture, American University of Beirut, Beirut, Lebanon.
[c]Department of Biomedical Sciences and Center for Craniofacial Research and Diagnosis, Texas A&M University College of Dentistry, Dallas, Tex.
[d]University of Pennsylvania, Philadelphia, Pa.
All authors have completed and submitted the ICMJE Form for Disclosure of Potential Conflicts of Interest, and none were reported.
Funding: Intramural research funds from the American University of Beirut Faculty of Medicine (Tabourian Dentofacial Educational Fund, Division of Orthodontics and Dentofacial Orthopedics) and Maroun Semaan Faculty of Engineering and Architecture.
Address correspondence to: Makram J. Ammoury, Orthodontics/Dentofacial Orthopedics, Medical Center, American University of Beirut, PO Box 11-0236, Riad El-Solh, Beirut 1107 2020, Lebanon; e-mail, ma322@aub.edu.lb.
Submitted, April 2018; revised and accepted, September 2018.
0889-5406/$36.00

https://doi.org/10.1016/j.ajodo.2018.09.017

accurate approximations of physiologic responses in internal structures, such as the periodontal ligament (PDL) and the alveolar bone,[7] depending on the precision of the model. Moreover, it allows for the study of a homogeneous sample (eg, canine retraction) while controlling the study variables (eg, bone stiffness, level of force application).[8] The application of FE modeling in orthodontic research has typically consisted of subjecting a single 3-dimensional (3D) model to various loading simulations to highlight several aspects of orthodontic mechanics, such as stress distributions on archwires and TADs,[9] stress and strain distributions in biologic tissues (PDL, bone, teeth),[10-12] displacement magnitudes and directions,[13] ideal positionings of orthodontic appliances,[14] and conditions inducing root resorption.[7] However, for any similar clinical setup, individual variations in responses are observed, such as a slower or faster distal movement of a canine in the extracted space of a premolar under similar force amounts and directions. Accordingly, departure from singular models is needed, because the study of larger samples helps determine central tendencies and potential outliers.

Different factors could account for individual variations, including TAD positions, anatomy, physiology, and metabolism of the involved systems (bone, teeth, PDL). Extreme variations in the density of the trabecular and cortical bones in the interradicular areas of dentate maxillae were found on computed tomographic (CT) scans.[15,16] The role of cortical bone in hindering tooth movement has been shown as a general determining factor, but not in the context of common tooth movements such as the distalization of molars or premolars with the use of TADs. The only FEA studies that have dealt with distalization modalities against mini-implants were on singular models and based on dentoforms rather than radiographs,[12,13,17] warranting further investigation in a system that mirrors variations of maxillary anatomy.

The aim of the present study was to compare the stress levels on the PDL of the buccal maxillary teeth in different set-ups of distalization with the use of miniscrews while taking into account individual variations in the anatomy of the maxilla and the biomechanical characteristics of the bone.

MATERIAL AND METHODS

The study protocol was approved by the American University of Beirut institutional review board. A 3D model was generated from a CT scan (0.3 mm per pixel resolution) of an adult patient with full permanent dentition seeking radiologic assessment of the head at our medical center. Excluded in the selection of the scan were patients undergoing orthodontic treatment or exhibiting the following features: malaligned, missing, or extracted teeth; deciduous teeth; craniofacial anomalies (eg, cleft lip or palate); or any medical condition affecting the maxilla or bones in general. To create the 3D model, the DICOM file images were imported and segmented with the use of ScanIP 7.0 (Simpleware, Exeter, U.K.). Masks of teeth, PDL, and cortical and cancellous bones were created based on their respective Hounsfield units (HU), and were further refined with the use of automated and manual tools. The PDL thickness was set at 0.25 mm, in line with previous reports.[10,14] Orthodontic appliances were sketched in Autodesk 3ds Max Design software (San Rafael, Calif) reproducing commercially available brackets and miniscrews. The latter were set at 6 mm in length and 1.5 mm in diameter, and were positioned between the second premolar and first molar with the head 5 mm from the archwire and angulated 30° with the use of the +CAD add-on module (Simpleware).

Anatomic variations of cortical bone stiffness and thickness were introduced in the initial model to replicate the bone characteristics of human cadavers studied for bone properties of the dentate maxilla by Peterson el al.[18] Those authors harvested cylindric bone specimens 4 mm in diameter from the crania of 15 dentate cadavers with a median age of 58.9 years. To preserve the material properties of the bone, the crania were frozen at −10°C shortly after death and maintained in a fresh unembalmed condition.[19,20] Trabecular bone was ground from the inner aspect of the cortical plate. The bone cylinder thickness of each prepared bone specimen was measured with the use of a digital caliper. Material property testing was performed using the pulse transmission technique[21] modified for craniofacial bone.[19] In the present study, because of missing thickness and stiffness data for some cadavers in the Peterson et al study,[18] the original data from 11 cadavers were analyzed to assess the effects of variation in bone stiffness and data from 12 cadavers were included in the analysis of thickness variation.

The 3D model was modified to divide the right side of cortical bone mask into 7 areas of interest (4 buccal and 3 palatal areas) matching the classification by Peterson et al.[18] and then assigned the stiffness of the various cadavers (Fig 1, *A-D*). Subsequently, the cortical bone thicknesses of the cadavers were incorporated into the template model used for stiffness variation. First, the average of a minimum of 200 cortical bone thickness measurements made at 9 different sites in each of the 7 bone parts determined the template model thickness. Next, the deformation (expansion or reduction) of each cortical bone part was calculated as the difference between the template model thickness and each model

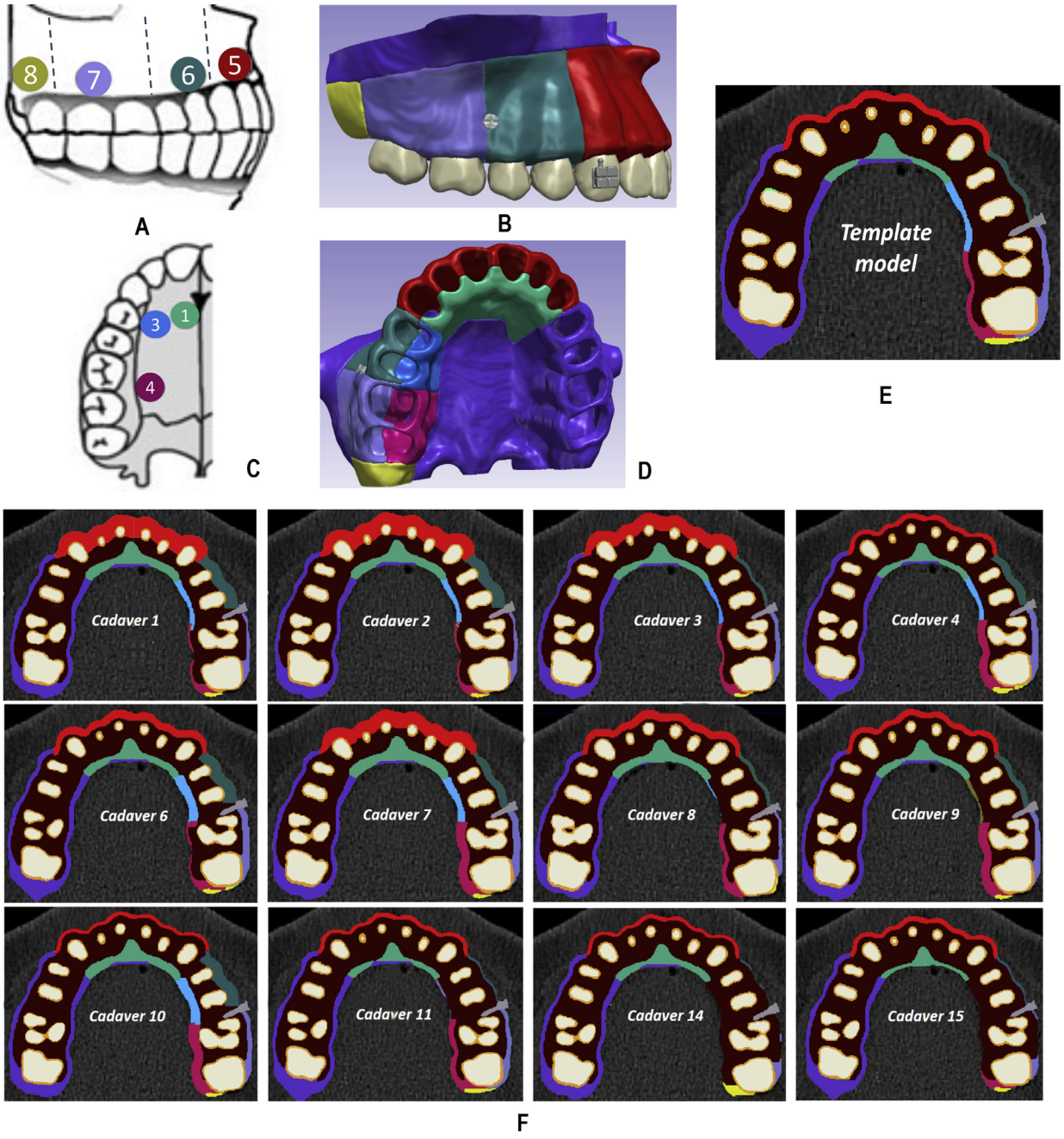

Fig 1. A-D, Dentate maxilla in which cortical bone was divided into 7 areas by Peterson et al[18] and the corresponding integration of these areas in the present study's 3D model. **A** and **C** adapted from Peterson et al.[18] **A,** Lateral view illustrating buccal cortical bone areas (*#5-8*). **B,** Corresponding modeling of the buccal areas. **C,** Occlusal view showing palatal cortical areas 1, 3, and 4. **D**, Corresponding modeling of the palatal areas. **E,** Axial cut at the level of the TAD in the original template model; **F,** Similar cuts of individualized models corresponding to 12 cadavers with modified cortical bone thicknesses. Variations in thickness are noted at various levels (eg, thinner bone palatal to the left first and second molars in #2 compared with thicker equivalent bone in #9). Areas: 1: *light green*, palatal cortical bone (CB) at incisors/canine region; 3: *blue*, palatal CB at level of premolars; 4: *fuchsia*, palatal CB at molars level; 5: *red*, buccal CB at incisors/canine region; 6: *dark green*, buccal CB at premolars level; 7: *purple*, buccal CB at level of molars; 8: *yellow*, CB at the tuberosity. Area 2 is outside of the frame of interest for the study.

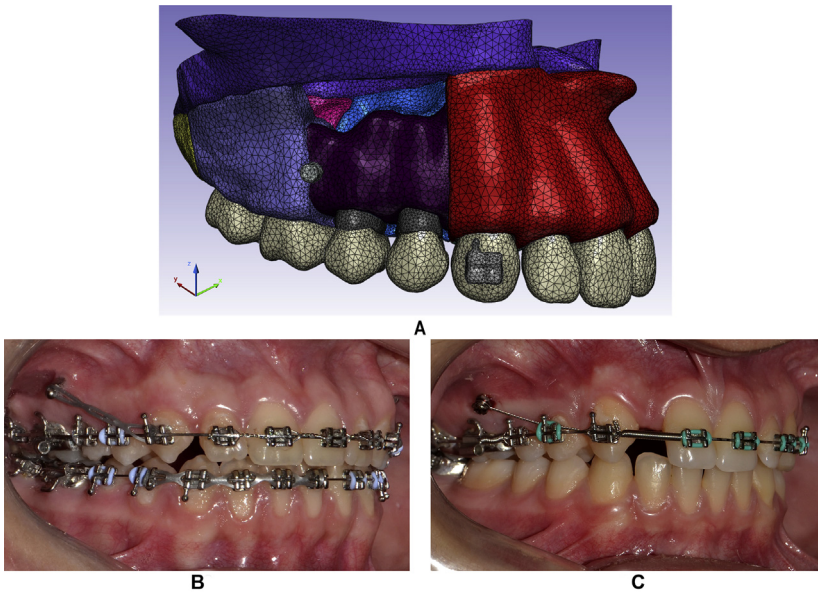

Fig 2. A, Meshed template model. Area 6 is removed to show the tissues behind the buccal cortical bone (CB): trabecular bone (*dark purple*), palatal CB at level of premolars (*blue*) and molars (*fuchsia*), and PDL of premolars (*dark gray*). **B, C,** Clinical photographs illustrating the simulated loading scenarios of direct anchorage modality (**B,** pull from TAD to canine) and indirect anchorage modality (**C,** open coil between first molar and second premolar, stainless steel ligature from TAD to canine).

(cadaver) thickness. This differential was translated by pixel addition or subtraction from the trabecular bone with the use of the dilate/erode tool in the ScanIP software. As a result, 12 new 3D models corresponding to 12 cadavers were generated (Fig 1, *E* and *F*).

The template model, on which the stiffness values from 11 cadavers would be tested, and the 12 models with thickness variations were meshed with the use of specialized software (+FE add-on module; Simpleware). The input files were exported to Abaqus (2011; Dassault Systèmes, Providence, RI). The template FE model comprised a total of 1,060,040 tetrahedral elements and 208,031 nodes (Fig 2, *A*). Trabecular bone, PDL, teeth, brackets, and miniscrews were assigned homogeneous isotropic material properties from available data in the literature that are commonly justified and used in orthodontic FEA studies[6,22-24] (Table I). Orthotropic material properties from individual cadavers were assigned for cortical bone.

Two loading set-ups were modeled: (1) direct anchorage, in which a force of 150 g was simulated from the miniscrew to the canine bracket; and (2) indirect anchorage, whereby 2 opposite forces (150 g each), applied against the first molar and second premolar, simulated an open coil while a pinned boundary condition applied on the canine bracket simulated the action of a metallic ligature placed from the miniscrew to the canine to negate the unwanted mesial force (Fig 2, *B* and *C*). Fixed boundary conditions were applied to the upper and posterior regions of the maxilla. Translational degrees of freedom were constrained to simulate the action of the brackets and archwires. Surface-to-surface interactions between adjacent teeth were used to model the contact interfaces. The contacts between the teeth were assumed to be frictionless.

Table I. Material properties applied to the various components of the model

Component	*Young modulus (MPa)*	*Poisson ratio*
Teeth	20 000	0.3
PDL	0.68	0.45
Trabecular bone	1500	0.33
Cortical bone	Variable	Variable
Brackets/TAD	200 000	0.3

Field et al, 2009[22]; Kojima et al, 2012[23]; Lim et al, 2003[24]; Tanne et al, 1987[6].

Stress and displacement data were collected on the canine, premolars, and molars. For stress data, average stresses (von Mises) of sets containing at least 150 randomly selected elements were reported from each of the buccal, palatal, mesial, and distal surfaces of the PDL. Von Mises stress is a measure of the elasticity of a material and represents the point at which the elastic

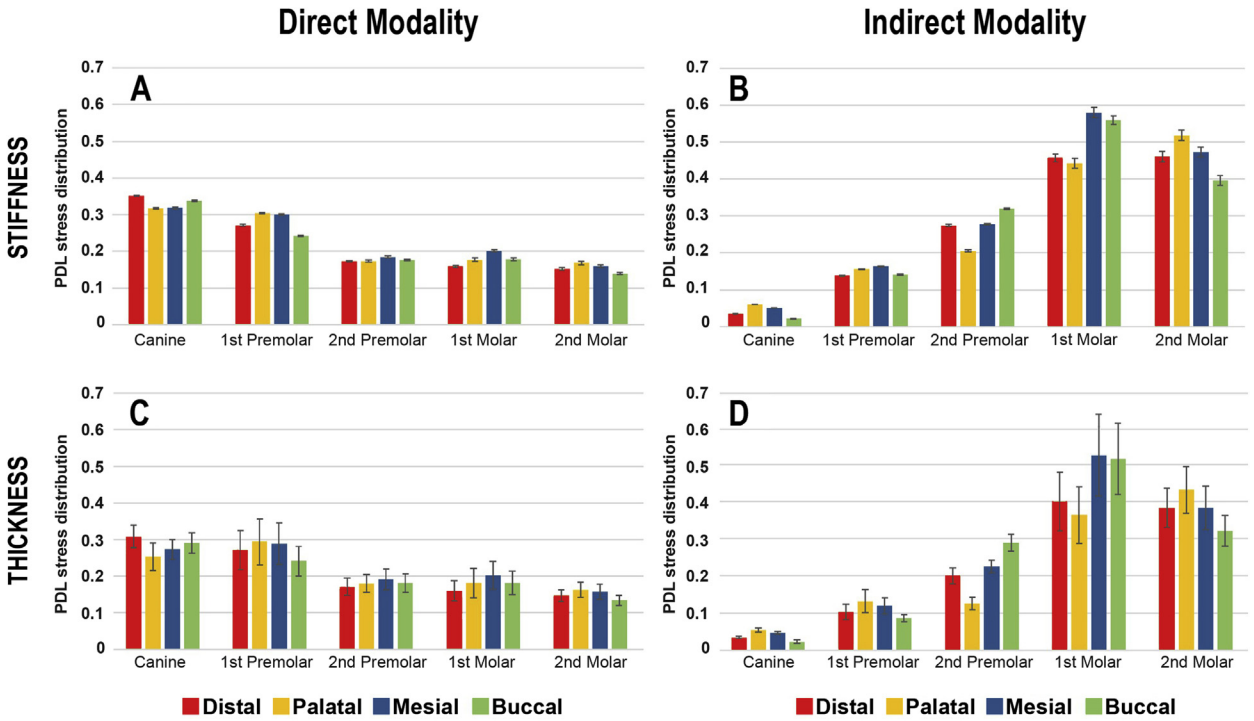

Fig 3. Stress distribution (von Mises in Pa) on the various surfaces of buccal teeth (canine to second molar) under stiffness (**A, B**) and thickness (**C, D**) variations and in the direct (**A, C**) and indirect (**B, D**) anchorage methods. Stresses followed similar patterns with changes in stiffness and thickness: highest at the canine and first premolar in the direct modality and at the molars in the indirect modality.

limit is exceeded and permanent deformation results. Displacements were collected from node sets containing at least 10 nodes from the centroid of each crown. The 3D coordinates were based on the occlusal plane: *x* (transverse plane), *y* (anteroposterior plane), and *z* (vertical plane). Positive values for *x*, *y*, and *z* indicated palatal, distal, and upward displacements, respectively (Fig 2, *A*).

In addition to descriptive statistics, analysis of variance (ANOVA) was used to compare the stresses between the different teeth at all surfaces, followed by Bonferroni post hoc analyses for multiple comparisons. Homogeneity of variances was tested for each set of comparisons, and when violated, Welch robust ANOVA and Games-Howell post hoc tests were reported instead. The Pearson product moment correlation coefficient was performed to test correlations between the stresses at the mesial, distal, buccal, and palatal parts of the PDL of each tooth with the thickness and stiffness of the corresponding palatal and buccal cortical bone areas. The Pearson correlation also was used to test correlations among the stresses recorded at the mesial surface and displacements (in every direction and total) at each tooth. SPSS statistical software was used for the statistical analyses.

RESULTS

Stress values were similar on all surfaces (mesial, distal, buccal, palatal) corresponding to the same tooth. However, in the indirect anchorage group, greater stress was measured on the buccal and mesial surfaces of the first molar compared with the distal and palatal surfaces, and lower stress on the palatal surface of the second premolar (Fig 3). Greater standard deviation values were observed in the models comparing cortical thickness variations than in those comparing stiffness variations.

In both anchorage modalities, stress distributions on each tooth were parallel in the thickness and stiffness variations. PDL stress was nearly equal in percentage at the canine in the direct (30%) and the molar in the indirect (36%) modalities. However, whereas the stress distributions in the direct modality decreased to nearly one-half of the amount registered on the canine at the level of the second premolar and molars, in the indirect modality stress values diminished progressively to nearly

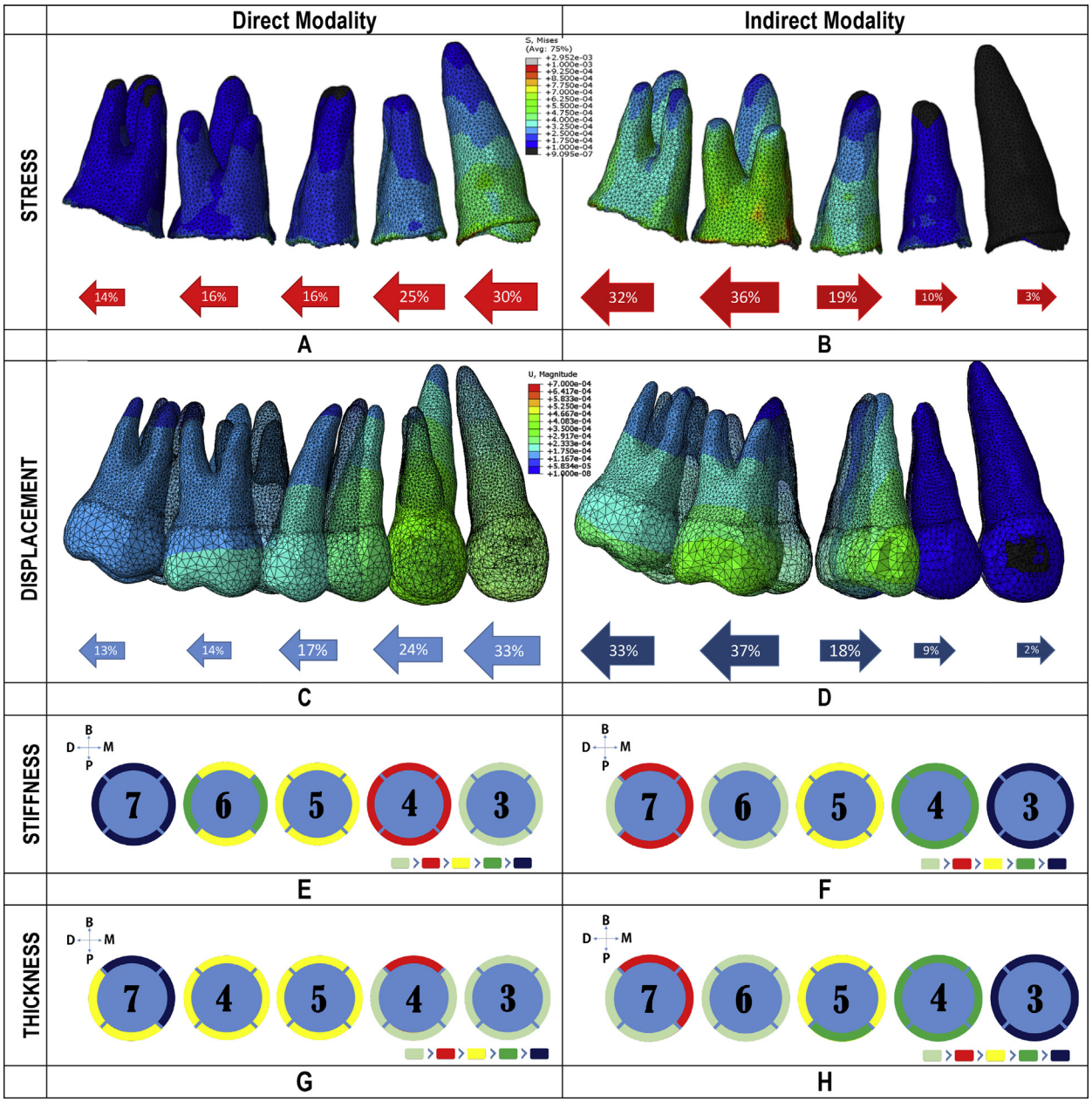

Fig 4. Von Mises stress distribution at PDL. **A,** Direct anchorage modality; **B,** Indirect anchorage modality (highest stress indicated in grey, lowest stress in black). Magnified displacements in (**C**) direct and (**D**) indirect anchorage modalities (greatest displacement in red; lowest in blue). **E-H,** Graphic representation of stress differences/similarities between surfaces of maxillary buccal teeth: stiffness variation in (**E**) direct and (**F**) indirect anchorage; thickness variation in (**G**) direct and (**H**) indirect anchorage. *Gray* indicates higher severity, *dark blue* lower severity. Note different gradients of stress on adjacent teeth with stiffness variations and similar colors between same surfaces of adjacent teeth with thickness variations. *3*, canine; *4*, first premolar; *5*, second premolar; *6*, first molar; *7*, second molar; *B*, buccal; *D*, distal; *M*, mesial; *P*, palatal surface of teeth.

one-half at the first premolar and almost nil at the canine (3%), which was originally set up as stationary (Fig 4, *A* and *B*). Displacement mirrored the progression of percentages in stress distribution in both direct and indirect modalities (Fig 4, *C* and *D*). On all teeth, higher stresses were registered at the coronal part of the PDL

Table II. Correlations between PDL stress recorded on the canine and first molar and bone properties (thickness and stiffness) at the corresponding palatal and buccal cortical bone regions in both distalization modalities

	Direct anchorage modality				*Indirect anchorage modality*			
Tooth surface	*D*	P	*M*	*B*	*D*	P	*M*	*B*
Cortical bone thickness								
P can	0.151	0.006	0.099	0.161	−0.064	0.253	0.113	−0.254
B can	0.072	0.022	−0.076	0.093	0.003	−0.226	−0.225	−0.313
P mol	0.28	0.135	0.292	0.308	0.298	0.291	0.262	0.291
B mol	0.384	0.114	0.286	0.294	0.289	0.177	0.287	0.286
Cortical bone stiffness								
P can	−0.134	−0.124	−0.097	−0.173	−0.134	−0.036	−0.114	−0.116
B can	0.077	−0.155	0.239	0.253	0.057	−0.267	0.012	0.457
P mol	−0.553	−0.536	−0.538	−0.561	−0.603* (0.049)	−0.586	−0.599	−0.585
B mol	−0.687* (0.019)	−0.720* (0.012)	−0.725* (0.012)	−0.700* (0.016)	−0.816† (0.002)	−0.813† (0.002)	−0.822† (0.002)	−0.808† (0.003)

Von Mises stress of the right canine and first molar at: *B*, buccal; *D*, distal; *M*, mesial; and *P*, palatal surfaces. Cortical bone properties at: *P can*, palatal canine/incisor area; *B can*, buccal canine/incisor area; *P mol*, palatal molar area; and *B mol*, buccal molar area. *P* values are given in parentheses for significant correlations; *$P \leq 0.05$; †$P \leq 0.01$.

compared with the apical part. Similarly, the displacements were greater at the crown level.

On stiffness variation, stresses were statistically significantly different between the same surfaces of adjacent teeth (Fig 4, *E* and *F*) in both distalization modalities. The only exceptions to this pattern were the palatal and buccal surfaces of the second premolar and the first molar in the direct anchorage modality, and the distal surfaces of the first and second molars in the indirect anchorage modality. Under thickness variation, more similarities were found between same surfaces of adjacent teeth in both distalization modalities. In the direct anchorage modality, no statistically significant differences were observed in the stress values among the distal, palatal, and mesial surfaces of the first premolar and canine or among all surfaces of the second premolar, first molar, and the distal and palatal surfaces of the second molar (Fig 4, *G* and *H*). Therefore, the stress amounts stopped decreasing past the second premolar. In the indirect anchorage modality, no statistically significant differences were observed between the palatal surfaces of the first and second premolars or between the distal and palatal surfaces of the first and second molars.

In both distalization modalities, low or no significant correlations were found between the stress values at either the canine or the first molar and the corresponding buccal and palatal cortical bone thicknesses (Table II). Also, low or no significant correlations were observed between the stresses at the canine and stiffness of the corresponding buccal and palatal cortical bone areas. However, at the first molar, significant correlations existed between stress amounts on all surfaces, mostly with buccal cortical bone stiffness (direct modality: $-0.68 < r < -0.72$; indirect modality: $-0.80 < r < -0.82$; $P < 0.05$). All correlations were negative, denoting the association of high stress with low stiffness.

Significant positive correlations were present between the average stresses and the total displacements of buccal teeth under direct anchorage ($r > 0.82$; $P < 0.05$). While high positive correlations existed between stress and displacement along the *y* and *z* axes, negative correlations were observed in the *x* axis (Table III). Similarly, in the indirect anchorage modality, significantly high correlations ($r > 0.95$; $P < 0.001$) were found between mesial stress at the second premolar and molars and the total displacement of these teeth. Slightly lower significant correlations ($r = 0.75$; $P = 0.007$) existed at the first premolar; no significant correlations were found at the canine. Negative correlations were observed between the stresses and the total displacements and the displacement in the *y* axis for the premolars and canine, while positive correlations were observed at the molars.

DISCUSSION

Most previous FEA studies were applied on a single model representing 1 clinical situation and with segmented elements of anatomy, thereby limiting the interpretation of results. In a novel approach, we accounted for individual variations by incorporating cortical bone stiffness and thickness derived from studies of cadavers into a complete 3D model, thus simulating variations existing between real patients. In addition, the complex maxillary anatomy was modeled to

Table III. Correlation between stress amounts at the mesial surfaces of every tooth and the corresponding displacements in the direct and indirect modalities

	Direct anchorage modality				*Indirect anchorage modality*			
Tooth	*U*	*Ux*	*Uy*	*Uz*	*U*	*Ux*	*Uy*	*Uz*
M3	0.864‡	−0.875‡	0.872‡	0.800†	−0.438	0.508	−0.508	0.222
M4	0.821†	−0.821†	0.820†	0.827†	−0.756†	0.759†	−0.759†	−0.732*
M5	0.930‡	−0.950‡	0.944‡	0.863‡	−0.957‡	0.959‡	−0.962‡	−0.827‡
M6	0.982‡	−0.982‡	0.982‡	0.957‡	0.997‡	−0.997‡	0.997‡	0.997‡
M7	0.987‡	−0.981‡	0.986‡	0.315	0.998‡	0.936‡	0.998‡	0.998‡

M, mesial von Mises stress; *U*, total displacement; *Ux*, displacement in transverse plane; *Uy*, displacement in anteroposterior plane; *Uz*, displacement in vertical plane; *3*, canine; *4*, first premolar; *5*, second premolar; *6*, first molar; *7*, second molar.
*$P \leq 0.01$; †$P \leq 0.007$; ‡$P \leq 0.001$.

reproduce the nonhomogeneous nature of the cortical bone in the buccal and palatal regions below the nasal floor, each region having specific physical characteristics that affect biomechanical performance, namely, stiffness, which is anisotropic (varying in magnitude in different directions), and thickness. To date, this approach is the closest to linking these characteristics with actual clinical situations.

As expected, tipping movements were predominant with both modalities, owing to the higher stress values and displacements at coronal levels than at apical regions (Fig 4, *A* and *D*). With variations in bone stiffness, stresses were different on adjacent teeth; in contrast, stresses tended to be similar between adjacent teeth when thicknesses were varied (Fig 4, *E* and *H*). Cortical bone thickness variation had less impact than stiffness variation on the initial displacements. This result is also supported by finding that bone stiffness (particularly on the buccal side) had significantly inverted correlations with stress values on different areas of the molar (Table II). In comparison, correlations between stress and thickness at the canine and molar were nearly absent.

These outcomes suggest that as long as the tooth encounters the stiffer area of the cortical bone, tooth movement is affected regardless of bone thickness. Rather than negating the importance of bone thickness, this finding would suggest that a thin but stiff layer of compact bone represents enough resistance to tooth movement. Additional resistance would be encountered if the tooth was moved through a thicker cortex. The immediate clinical implication would be to steer a tooth away from compact bone, if possible, and accomplish its movement in a trough of trabecular bone that has less density and stiffness. Alternate treatment plans might be considered, such as the extraction of the premolars instead of molar distalization.

Under direct anchorage, an optimal force of 150 g resulted in low stresses and displacements at the molars, which may not be efficient or may translate into slower movement (Fig 4, *A* and *C*), indicating the need of a heavier force for the initial molar movement. Park et al[1] considered that a greater force of 200 g was not excessive when used for direct anchorage group distal movement of teeth. They calculated that such force provided ~30 g per tooth, which is considered to be light compared with ordinary orthodontic forces. Therefore, the correspondence and efficiency of force amount with variations in stiffness and thickness of the compact bone also should be further investigated. With indirect anchorage, stresses (19%) and displacements (18%) at the second premolar, subjected to the same amount of force (150 g), were nearly half of those at the molars (Fig 4, *B* and *D*), suggesting that the restraining force on the canine should be at least equal to the reaction on the premolars. Accordingly, a positive force through an elastomeric chain or open coil would be applied against the canine rather than a passive tie.

These interpretations are plausible, despite the lack of explicit corroborating clinical research. In fact, the literature on modalities of distalization with the use of TADs mainly covers separate advocacies of either the direct or the indirect modality, with few comparisons of both within a single project. Most reports include the placement of miniscrews in the palate in conjunction with distalization appliances[25-27]; fewer studies describe buccally placed TADs.[1,28-30] Disparities among studies are likely associated with anatomic and therapeutic conditions, such as the distalization forces (from 150 g[29] to 400 g[27]), treatment duration (4.6 months to 11.2 months[27]), and the number of patients with second molars present (13.6% to 100%[31]). Interestingly, the monthly rates of tooth movement were similar across most studies: from 0.5 mm to 0.9 mm.[25] While our research complements clinical investigation because it targets the role of the cortical bone in the distalization process, it also controls for other local variables in silico (on computer simulations). This role cannot be investigated clinically.

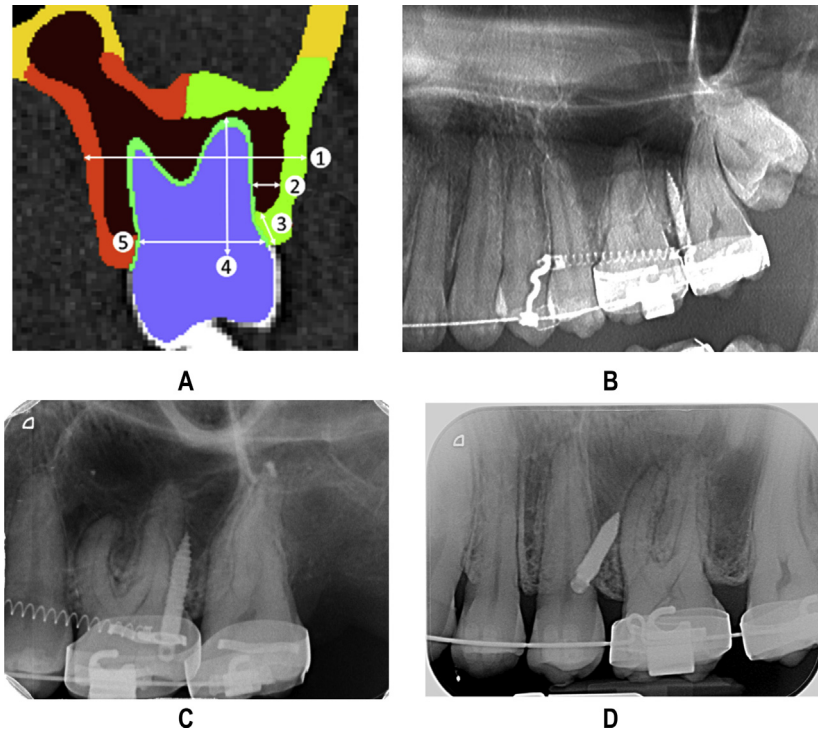

Fig 5. A, Anatomic factors affecting dental displacement (in frontal view): *1*, width of the alveolus; *2*, distance from molar root to cortical bone; *3*, height of the cortical bone; *4*, height of the molar root; *5*, width of the molar. **B-D,** Radiographic images showing (in sagittal views) anatomic obstacles that limited distal movement in an adult patient: presence of third molar (**B**) that was extracted (**C**), root morphology (**B, C**), low sinus (**B, C**), cortical bone height between first and second molars and between second premolar and first molar.

The results underscore the importance of the relationship between the roots of the teeth and the corresponding cortical bone in defining a successful distalization within an acceptable period of time and without side-effects (eg, undue tooth tipping, root resorption). Accordingly, local anatomic factors influencing the root-cortex interface should be assessed, including the width of the alveolus, root-cortex distance, height of the coronal cortical bone in contact with the PDL, and the buccolingual width of the molar (Fig 5, *A*). Other potential barriers to molar distalization include sinus proximity or invagination, root morphology, and the third molars (Fig 5, *B-D*). These local features may require evaluation through 3D radiographic imaging to guide treatment planning (extraction or nonextraction) and mechanotherapy (direct or indirect distalization). When low resistance to distalization is encountered, direct anchorage and other modalities would succeed. In the presence of high resistance, in-course treatment modifications may be required to overcome the anatomic barriers, such as shifting to sequential distalization (molar movement followed by other teeth) instead of increasing force magnitude.

This study provides a "snap-shot" view of the initial stresses and displacements within the model when the tooth is pushed into the PDL space; it does not depict changes that occur over time, such as bone remodeling (bone resorption and apposition), healing, or friction. Subsequent clinical results may not be similar to the initial response. A change in the onset and rate of tooth movement may normally occur, as indicated through a recorded decrease in the rate of molar protraction from 0.60 mm to 0.33 mm per month during the first 8 months of treatment.[32] The time-dependent (continuous/dynamic) FE approach[9,31] should help in exploring such changes to yield accurate mathematical simulations of the biologic processes of tooth movements over time (including the PDL and bony reactions).[9,31] Actual clinical data would be entered into the research model to generate information on biomechanical responses of teeth and bone during orthodontic treatment that would eventually help to develop controlled personalized mechanotherapy, planned according to

the subject's anatomy to achieve preset goals and minimize side-effects.

CONCLUSIONS

1. With the use of a novel approach to FEA that integrated human data of cortical bone properties to account for individual variations in maxillary structure, the results suggested that variations in cortical bone stiffness represent the primary influence on tooth movement. Accordingly, the interface between the teeth being moved and corresponding cortex affects the success of molar distalization.
2. Generic preferences for direct or indirect distalization are not appropriate, because local morphologic individual characteristics may dictate one or the other in personalized treatment. Research should be focused on the anatomic conditions under which one approach is preferable to the other.

ACKNOWLEDGMENTS

The authors thank Dr. Maria Saadeh for the statistical analyses, Dr. Georges Ayyoub for his helpful insight and feedback and Rakan Ammoury and Rawad Hayek for their assistance in data collection.

REFERENCES

1. Park H-S, Lee S-K, Kwon O-W. Group distal movement of teeth using microscrew implant anchorage. Angle Orthod 2005;75:602-9.
2. da Costa Grec RH, Janson G, Branco NC, Moura-Grec PG, Patel MP, Henriques JFC. Intraoral distalizer effects with conventional and skeletal anchorage: a meta-analysis. Am J Orthod Dentofacial Orthop 2013;143:602-15.
3. Arcuri C, Muzzi F, Santini F, Barlattani A, Giancotti A. Five years of experience using palatal mini-implants for orthodontic anchorage. J Oral Maxillofac Surg 2007;65:2492-7.
4. Papadopoulos MA, Tarawneh F. The use of miniscrew implants for temporary skeletal anchorage in orthodontics: a comprehensive review. Oral Surg Oral Med Oral Pathol Oral Radiol Endod 2007;103:e6-15.
5. Wiechmann D, Meyer U, Büchter A. Success rate of mini- and micro-implants used for orthodontic anchorage: a prospective clinical study. Clin Oral Implants Res 2007;18:263-7.
6. Tanne K, Sakuda M, Burstone CJ. Three-dimensional finite element analysis for stress in the periodontal tissue by orthodontic forces. Am J Orthod Dentofacial Orthop 1987;92:499-505.
7. Kamble RH, Lohkare S, Hararey PV, Mundada RD. Stress distribution pattern in a root of maxillary central incisor having various root morphologies: a finite element study. Angle Orthod 2012;82:799-805.
8. Viecilli R. Self-corrective T-loop design for differential space closure. Am J Orthod Dentofacial Orthop 2006;129:48-53.
9. Ammar HH, Ngan P, Crout RJ, Mucino VH, Mukdadi OM. Three-dimensional modeling and finite element analysis in treatment planning for orthodontic tooth movement. Am J Orthod Dentofacial Orthop 2011;139:e59-71.
10. Sung S-J, Jang G-W, Chun Y-S, Moon Y-S. Effective en-masse retraction design with orthodontic mini-implant anchorage: a finite element analysis. Am J Orthod Dentofacial Orthop 2010;137:648-57.
11. Çifter M, Saraç M. Maxillary posterior intrusion mechanics with mini-implant anchorage evaluated with the finite element method. Am J Orthod Dentofacial Orthop 2011;140:e233-41.
12. Yu I-J, Kook Y-A, Sung S-J, Lee K-J, Chun Y-S, Mo S-S. Comparison of tooth displacement between buccal mini-implants and palatal plate anchorage for molar distalization: a finite element study. Eur J Orthod 2014;36:394-402.
13. Sung E-H, Kim S-J, Chun Y-S, Park Y-C, Yu H-S, Lee K-J. Distalization pattern of whole maxillary dentition according to force application points. Korean J Orthod 2015;45:20-8.
14. Nihara J, Gielo-Perczak K, Cardinal L, Saito I, Nanda R, Uribe F. Finite element analysis of mandibular molar protraction mechanics using miniscrews. Eur J Orthod 2015;37:95-100.
15. Lindh C, Obrant K, Petersson A. Maxillary bone mineral density and its relationship to the bone mineral density of the lumbar spine and hip. Oral Surg Oral Med Oral Pathol Oral Radiol Endod 2004;98:102-9.
16. Chugh T, Ganeshkar SV, Revankar AV, Jain AK. Quantitative assessment of interradicular bone density in the maxilla and mandible: implications in clinical orthodontics. Prog Orthod 2013;14:1.
17. Kang J-M, Park JH, Bayome M, et al. A three-dimensional finite element analysis of molar distalization with a palatal plate, pendulum, and headgear according to molar eruption stage. Korean J Orthod 2016;46:290-300.
18. Peterson J, Wang Q, Dechow PC. Material properties of the dentate maxilla. Anat Rec A Discov Mol Cell Evol Biol 2006;288:962-72.
19. Schwartz-Dabney CL, Dechow PC. Variations in cortical material properties throughout the human dentate mandible. Am J Phys Anthropol 2003;120:252-77.
20. Zioupos P, Currey J. Changes in the stiffness, strength, and toughness of human cortical bone with age. Bone 1998;22:57-66.
21. Ashman R, Cowin S, Van Buskirk WC, Rice JC. A continuous wave technique for the measurement of the elastic properties of cortical bone. J Biomech 1984;17:349-61.
22. Field C, Ichim I, Swain MV, et al. Mechanical responses to orthodontic loading: a 3-dimensional finite element multi-tooth model. Am J Orthod Dentofacial Orthop 2009;135:174-81.
23. Kojima Y, Kawamura J, Fukui H. Finite element analysis of the effect of force directions on tooth movement in extraction space closure with miniscrew sliding mechanics. Am J Orthod Dentofacial Orthop 2012;142:501-8.
24. Lim JW, Kim WS, Kim IK, Son CY, Byun HI. Three dimensional finite element method for stress distribution on the length and diameter of orthodontic miniscrew and cortical bone thickness. Korean J Orthod 2003;33:11-20.
25. Fudalej P, Antoszewska J. Are orthodontic distalizers reinforced with the temporary skeletal anchorage devices effective? Am J Orthod Dentofacial Orthop 2011;139:722-9.
26. Cozzani M, Fontana M, Maino G, Maino G, Palpacelli L, Caprioglio A. Comparison between direct vs indirect anchorage in two miniscrew-supported distalizing devices. Angle Orthod 2016;86:399-406.
27. Mohamed RN, Basha S, Al-Thomali Y. Maxillary molar distalization with miniscrew-supported appliances in Class II malocclusion: a systematic review. Angle Orthod 2018;88:494-502.
28. Cornelis MA, De Clerck HJ. Maxillary molar distalization with miniplates assessed on digital models: a prospective clinical trial. Am J Orthod Dentofacial Orthop 2007;132:373-7.

29. Sugawara J, Kanzaki R, Takahashi I, Nagasaka H, Nanda R. Distal movement of maxillary molars in nongrowing patients with the skeletal anchorage system. Am J Orthod Dentofacial Orthop 2006;129:723-33.
30. ALee SK, Abbas NH, Bayome M, Baik UB, Kook YA, Hong M, Park JH. A comparison of treatment effects of total arch distalization using modified C-palatal plate vs buccal miniscrews. Angle Orthod 2018;88:45-51.
31. Hamanaka R, Yamaoka S, Anh TN, Tominaga JY, Koga Y, Yoshida N. Numeric simulation model for long-term orthodontic tooth movement with contact boundary conditions using the finite element method. Am J Orthod Dentofacial Orthop 2017;152:601-12.
32. Roberts WE, Arbuckle GR, Analoui M. Rate of mesial translation of mandibular molars using implant-anchored mechanics. Angle Orthod 1996;66:331-8.